International Journal of Non–Linear Mechanics 88 (2017) 11–20

Contents lists available at ScienceDirect

International Journal of Non–Linear Mechanics

journal homepage: www.elsevier.com/locate/nlm

Interaction between snap-through and Eulerian instability in shallow structures

F. Bazzucchi*, A. Manuello, A. Carpinteri

Politecnico di Torino, Department of Structural, Geotechnical and Building Engineering, Corso Duca degli Abruzzi 24, 10129 Torino, Italy

ARTICLE INFO

Keywords:
Structural stability
Snap-through
Buckling
Nonlinear analysis
Interaction analysis
Equilibrium path
Imperfection sensitivity
Coupled instability

ABSTRACT

The multifold nature of structural instability problems necessitates a number of different kinds of analytical and numerical approaches. Furthermore, instability collapses of large-span roof sensitized the global community to reduce the effects of geometrical imperfections, then some limiting recommendations have been recently proposed. This study provides new insights into the interaction between the two different categories of structural instability and, for the first time, a unified theoretical evaluation of the critical load due to interaction is proposed. The snap-through phenomenon of 2D Von Mises arches was investigated by an incremental-displacement nonlinear analysis. At the same time, the equilibrium paths were considered in relation to the Eulerian buckling loads for the same structural systems. For each structural scheme the effect of the two governing parameters was investigated: slenderness and shallowness ratios. For these purposes, several original theoretical and numerical snap-through versus buckling interaction curves were obtained. These curves provide indications about the prevailing collapse mechanism with regards to the geometric configuration of the structure. Consequently, this innovative method is able to predict the actual instability of a wide range of mechanical systems. With this approach, it is possible also to establish the connection between the magnitude of structural imperfections (defects) and instability behavior. The proposed procedure is able to provide the effective critical load given by the interaction effect and to correlate the instability behavior to the maximum tolerable imperfection sizes.

1. Introduction

Traditionally, in Civil Engineering, Eulerian buckling and snap-through instabilities are treated separately because they are supposed to take place with different modalities and physical mechanisms. However, such phenomena can interact in real structures implying more critical scenarios (*interaction*) than the ones obtained by separated analyses. One of the main consequences is that the greater the interaction the greater the imperfection sensitivity. A typical case where the interaction effect is appreciable is that of shallow structures – arches or domes – in which the presence and the magnitude of the interaction mainly depend on the slenderness and the shallowness ratios.

It has long been recognized that slender structures generally loses their stability by “snapping” or “buckling”. On one hand, from a theoretical point of view, the structure is said to snap when the equilibrium path, emerging from the unloaded state, loses its stability on yielding the first locally maximum value of the load. Commonly, this condition occurs when the structure works mostly through a compressive regime of internal forces. On the other hand, the theoretical critical condition is reached when the structure is said to buckle and the equilibrium path loses its stability at a point of bifurcation. The study of the latter condition reached a very complete treatment in the work of Koiter [1], who provided the fundamentals to determine the imperfection sensitivity of a structural system by the investigation of the pre-critical elastic buckling condition. This study represents the first step of a more refined and generalized theory on the elastic buckling. A theory that is rooted in the works of some of the most eminent scientists of the Eighteenth Century [2,3]. On the contrary, the snap-through instability, even if widely accepted, did not find rigorous mathematical collocation until the Sixties. Concerning this topic, in fact, the main contribution has been given by Thompson [4,5] where the analytical conditions in which snap-trough may occur are enounced theoretically. This author, founding his work on the expression of the total potential energy by series expansion, demonstrated that the limit point condition (*snap-through*) is related to a zero value of one of the coefficients of the expansion and, if two null coefficients are present, the bifurcation point is recognized. It is worth to note that this bifurcation occurs in a non-

* Corresponding author.
E-mail address: fabio.bazzucchi@polito.it (F. Bazzucchi).

http://dx.doi.org/10.1016/j.ijnonlinmec.2016.10.006
Received 8 April 2016; Received in revised form 12 September 2016; Accepted 16 October 2016
Available online 18 October 2016

linear regime, because the pre-critical deformations are not neglected. Thompson's theories find the natural prosecution in the works of Huseyin [6,7], who extended the definition of the instability conditions to the case of multiple independent loads. In order to do this, Huseyin used the definition of stability domains, because the nonlinear essence of the problems makes ineffective the use of superposition principle to obtain the equilibrium path of the structure. The obtained surface (a curve when only two independent parameters are considered) is the boundary over which the critical condition occurs. Working on these parameters, the nature of the instability (snap-through or buckling) cannot be recognized a priori, thus additional conditions must be defined aside the total potential energy definition [8,9].

These studies represent the fundamentals of a general theory on elastic stability and they have a remarkable importance since allow to handle the real systems (affected by imperfections) by the simple definition of a pre- deformed geometrical configuration in the Lagrangian equations. An appropriate example can be found in the work of Pecknold et al. [11].

In the last two decades, a consistent effort in how to evaluate the imperfection sensitivity of shallow and slender structures has been carried out by the scientific community. Operating this way, instability problems become primary and many optimization procedures (based on instability conditions) have been proposed. Among these studies, the coincidence of the critical loads related to different buckling modes has been proposed (*Bleich-Shanley postulate*) [10]. At the same time, the studies by Koiter, Thompson, and Huseyin demonstrated that interaction of different equilibrium paths could lead the system to an higher imperfection sensitivity. Finally, Gioncu [12] observed that in the real structures the presence of imperfections implies that the intersection between two equilibrium paths degenerates to a limit point. The greater the imperfection, the smaller the consequential critical load [12].

To this day, the study of snap-through of framed structures is carried out mostly in the field of deployable [13] and shape-changing systems [14], because new stable spatial configurations can be achieved by the occurrence of a snap instability. The so-called *buckling induced* systems have been recently proposed for MEMS devices [15], and they are based on the same concepts of shape-changing structures. For all these applications, the control of the displacements and (above all) of the actual maximum instability load is essential. Despite the fact that original researches about this topic are not so extended, some works have proposed new approaches on the study of the Von Mises truss [16] and some original derivations of it [17] to evaluate the actual displacements and instability loads.

In this paper, the investigation on the interaction between the two different categories of structural instabilities was presented and, for the first time, a unified theoretical evaluation of the critical load due to interaction was proposed. Moreover, the theories of Gioncu were confirmed even for the case of the interaction between the two different typologies of instability, snap-through and buckling. On the other hand, results demonstrated how the magnitude of the imperfections is not very significant with this type of interaction. To this purpose, the snap-through phenomenon of 2D Von Mises arches was investigated by an incremental-displacement nonlinear analysis. At the same time, the equilibrium paths were considered in relation to the Eulerian buckling loads for the same structural systems.

For each structural scheme, different parameters were analyzed, such as slenderness, together with arch depth. Several original theoretical and numerical snap-through versus buckling interaction curves were obtained. These curves provide indications about the prevailing collapse mechanism with regards to the geometric configuration of the structure. Consequently, this innovative method is able to predict the actual instability of a wide range of mechanical systems. With this approach, it is also possible to establish the relationship between the magnitude of the structural imperfections (defect) and instability behavior. The proposed procedure is able to provide the effective critical load given by the interaction effect and to correlate the instability behavior to the maximum tolerable imperfections. Therefore, this study makes a major contribution to research on non-linear instability of structures by demonstrating that the evaluation of the critical load can be affected by the interaction of different-order phenomena.

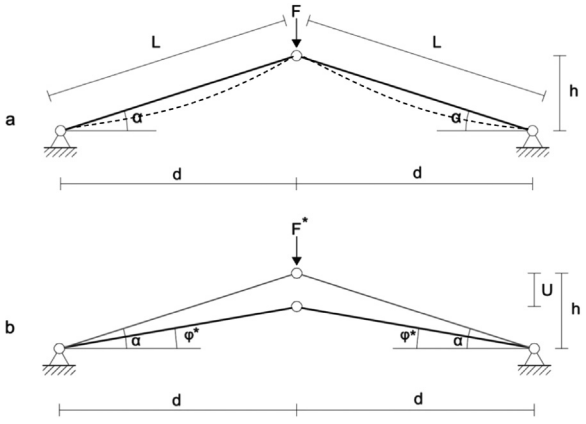

Fig. 1. a) Eulerian elastic buckling of a Von Mises Arch and the adjacent configuration (dotted lines). **b)** The generic equilibrium configuration along a displacement control analysis, identified by F^* and φ^*.

2. Interaction between elastic buckling and snap-through instability

2.1. Interaction in a simple structure

The mechanical system represented in Fig. 1a is traditionally called Von Mises Arch [18]. This simple structure is made of two hinged bars subjected to a vertical force F applied at the crown. As is well-known, the arch has a nonlinear pre-critical behavior, which involves a snap-through if the equilibrium path is followed beyond the limit point. This same system can be analyzed in respect to the elastic buckling, assuming a non-deformed pre-critical configuration. For a given external load F, the bars react with the axial forces:

$$N = \frac{1}{2}\frac{F}{\sin\alpha}. \tag{1}$$

When N reaches the critical Eulerian buckling load of a hinged bar in compression ($N_{CR,EB}$), the bars lose their flexural stiffness and the equilibrium is established in the adjacent configuration (see Fig. 1a). Under these conditions, the external load is equal to

$$\frac{1}{2}\frac{F}{\sin\alpha} = N_{CR,EB} = \pi^2\frac{EI}{L^2}, \tag{2}$$

$$F_{CR,EB} = 2\pi^2\frac{EI}{L^2}\sin\alpha. \tag{3}$$

In order to determine the more burdensome instability condition, this load must be compared to the snap-through instability load [4,19]:

$$F = 2EA\sin\varphi\left(1 - \frac{\cos\alpha}{\cos\varphi}\right), \tag{4}$$

in which the value of the critical angle φ_{CR} has to be substituted. This value was obtained by the functional analysis of the equilibrium path. Between the two related limit points, an unstable branch of the path (as indicated by the relative negative slope in Fig. 2) is identified, and the values of the critical angle are

$$\varphi_{1,2} = \pm\arccos\sqrt[3]{\cos\alpha}\,. \tag{5}$$

The limit points are obtained by findings the turning points of Eq. (4), since its zeros represent the equilibrium coordinate of the system.

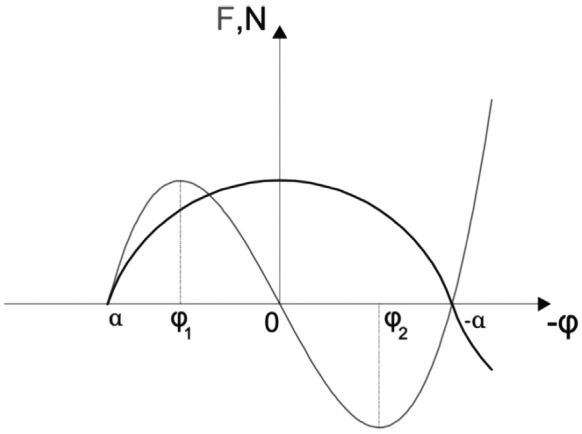

Fig. 2. Variation of the axial force in the generic bar along the equilibrium path (black curve) overlapped to the relative snap-through equilibrium path (grey).

Is it worth to note that, both the critical loads are dependent on the value of the initial angle α, which indicates the shallowness of the arch. This means, that for a given bar cross section, only the shallowness of the arch represents the discriminating factor between a snap-through instability or an elastic buckling one.

A complete analysis must consider both the two instability phenomena in order to choose the correct design scenario, by the selection of the minimum critical loads. Operating this way, however, the two instabilities typologies are treated in a separated way, thus their possible mutual interaction is neglected. In the aim of investigating this interaction, let us consider a generic configuration (φ^*,F^*) along the nonlinear equilibrium path before the limit point (Fig. 1b). Equilibrium in this configuration implicates that the value of the axial force is equal to

$$N = \frac{1}{2}\frac{F^*}{\sin\varphi^*}. \tag{6}$$

It is obvious that the nature of the problem leads to a larger value of the axial force in the deformed configuration in comparison to the one characterized by the initial angle α. Then, substituting (4) into (6), the axial force increases nonlinearly along the equilibrium path according to the following law:

$$N = EA\left(1 - \frac{\cos\alpha}{\cos\varphi}\right). \tag{7}$$

This relation was reported in Fig. 2 (black curve) in overlapping to the snap-through equilibrium path (grey). When the axial force reaches the Eulerian critical load $N_{CR,EB}$, the system undergoes through a bifurcation of equilibrium (Fig. 3). This point is characterized by a lower value of the external load with respect to the one obtained by (3). The bifurcation, occurring in nonlinear regime before the critical snap-through, takes place when the primary equilibrium path, given by Eq. (3), is intersected by the equilibrium path provided by the following equation:

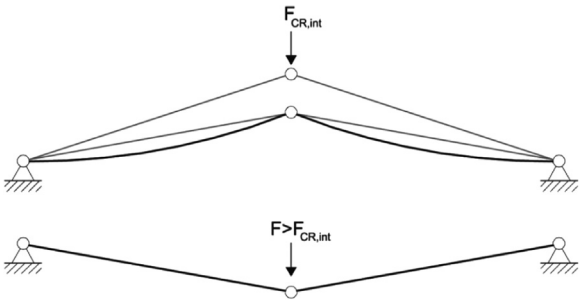

Fig. 3. Nonlinear bifurcation of equilibrium.

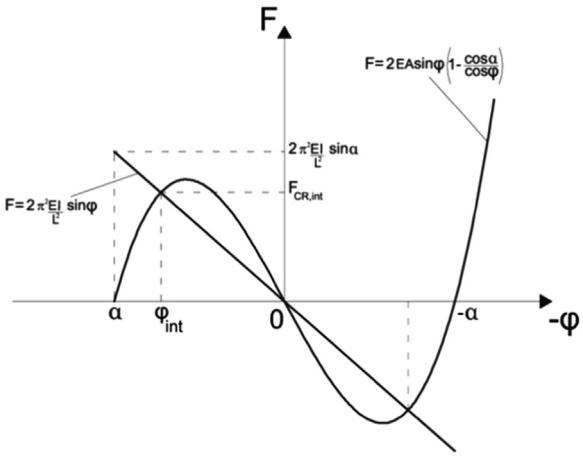

Fig. 4. Interaction angle φ_{int} and load $F_{cr,int}$ identified by the intersection between the primary snap-through equilibrium path and the Eulerian buckling path.

$$F = 2\pi^2\frac{EI}{L^2}\sin\varphi. \tag{8}$$

This equation was obtained by introducing the value of $N_{CR,EB}$ into (6). The intersection, represented in Fig. 4, occurs in a range $[\alpha;-\alpha]$ (coordinate axis is inverted since φ decreases along the path) of the coordinate system. In this domain the portion of sinusoidal Eq. (8) can be assimilated to a straight line due to small values of the shallowness angle α. Eq. (8) is a function defined in the range π; $-\pi$. By focusing on the point of intersection identified by the angle φ_{int}, the system lays in a mixed condition between the snap-through and the unstable buckling bifurcation: related branch is decreasing, thus a small perturbation would lead the structure to snap towards a non adjacent equilibrium configuration (Fig. 5a). Considering instead a displacement controlled test, a perturbation leads the system to abandon the primary equilibrium path towards the branched one and to follow it until the primary one is intersected again. Fig. 5b shows how the deflection at the mid-span of the two beams (subtracted by the constant vertical displacement of the primary equilibrium path) is present only along the bifurcation, that is where the beams are in equilibrium in a non-rectilinear configuration.

The interaction between the two instabilities occurs only if the intersection between the equilibrium paths is located before the critical state of the snap-through, identified by Eq. (6). There are four possible configurations for the equilibrium paths, and, only two of them make possible the interaction, cases a) and b) as shown in Fig. 6. Case c) in Fig. 6 shows that the system already snapped with the maximum critical instability load, $F_{CR,S\text{-}T}$. Once the snap-through limit point was overcome and the primary equilibrium path was intersected by the elastic buckling one, no interaction took place. As a limit case, if the elastic buckling load is very high with respect to the snap-through one, the slope of the correlated equilibrium path does not allow any intersection (Fig. 6d).

Existence interaction conditions depend on shallowness and slenderness of the structure. Recalling (7), which provides the axial force in the bars, and equalizing it to $N_{CR,EB}$ the following relation can be obtained:

$$1 - \frac{\cos\alpha}{\cos\varphi} = \frac{\pi^2}{\lambda^2}. \tag{9}$$

Substituting the value of φ given by (5), the intersection between the two equilibrium paths is forced to coincides with the snap-through limit point. The following equation, defined as *interaction curve*:

$$\alpha = \arccos\left(1 - \frac{\pi^2}{\lambda^2}\right)^{\frac{3}{2}} \tag{10}$$

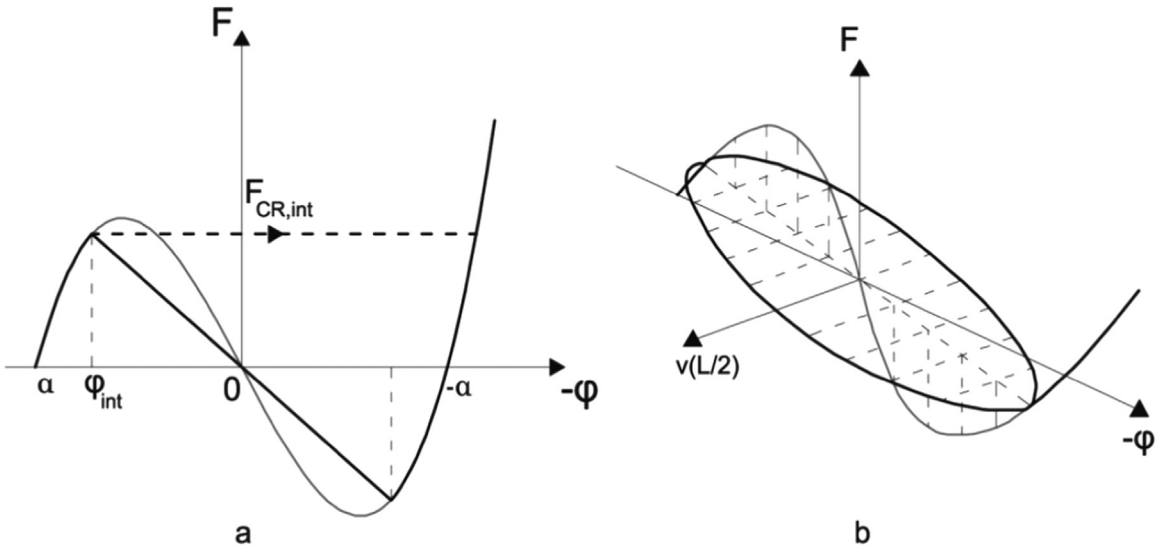

Fig. 5. a) Interaction equilibrium path with the nonlinear bifurcation unstable branch. **b)** Value of the vertical displacement at midspan of every beam along the nonlinear bifurcation branch.

indicates the value for slenderness λ so that, for a given shallowness α, the elastic buckling instability and the snap-through occur simultaneously. Analogously, Eq. (9) provides the angle φ_{int}, for which the interaction occurs:

$$\varphi_{\text{int}} = \arccos\left(\frac{\cos\alpha}{1-\frac{\pi^2}{\lambda^2}}\right). \tag{11}$$

A smaller value of φ_{int} than $\varphi_{1,2}$ (Eq. (5)) means that the interaction occurs because the snap-through critical state is located

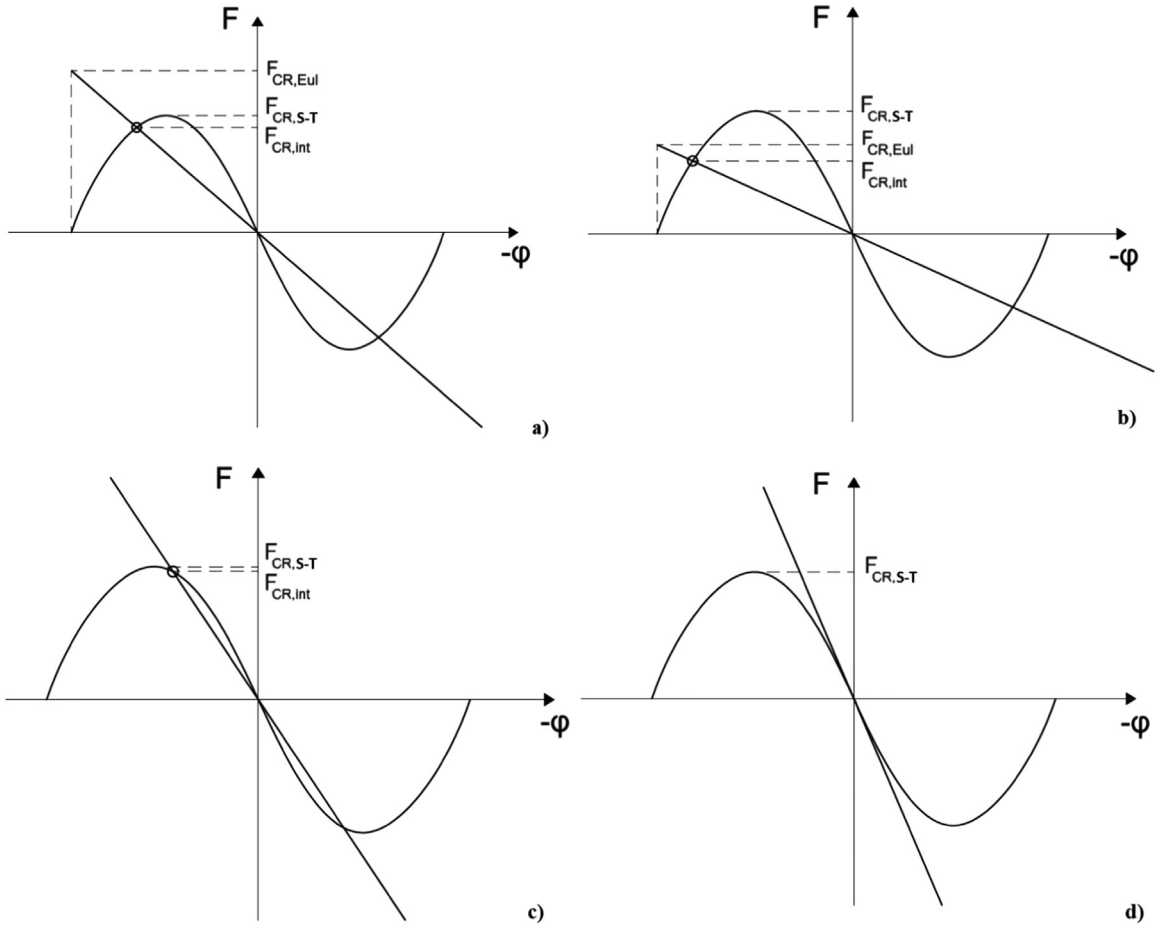

Fig. 6. Possible configurations of the equilibrium paths. **a)** and **b)** the interaction phenomenon is real since the intersection occur before the limit snap-through point. In **c)** the interaction occur along the already unstable branch of the primary path since the intersection is located beyond the limit point. In **d)** the interaction cannot take place because there is no intersection between the equilibrium paths.

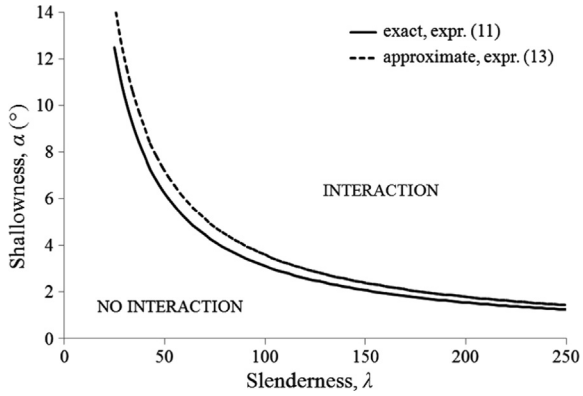

Fig. 7. Interaction curve for a Von Mises Arch.

later along the equilibrium path.

Relation (10) can be simplified with a linearization of Eqs. (4), (5) and (8), hypothesis which is valid for small shallowness ratio (α). Operating in this way, the approximate expression for Eq. (10) is:

$$\alpha \cong 2\frac{\pi}{\lambda}. \tag{12}$$

Plotting Eq. (10) and Eq. (12), as reported in Fig. 7, it is possible to observe that the linearization remains efficient until the shallowness is high, although provides adequate values also for larger values of α. The curves reported in Fig. 7 represent the boundary condition for which the interaction between the two instability typologies may or may not occur. For a given value of slenderness λ, if the shallowness ratio is adequate to define a couple (λ,φ) above the curves, then an interaction is present and its effect on load reduction is stronger as the distance from the curve increases (see Fig. 7). The value of the angle φ, which defines the critical deformed configuration, can be evaluated by Eq. (11). The critical interaction load can be obtained from every relation between φ and the external load, i.e. Eq. (8).

It is worth to note that all the obtained results are consistent with what has been presented in the existing literature for the stability of Von Mises arches [4,11,15,19].

Interaction between snap-through and elastic buckling, when it is present, implies a lower value of the critical load respect to the ones evaluated by the two separated analyses, as can be observed in Fig. 4. This reduction is consistent, and for typical slenderness and shallowness ratios, can reach the 40% of the maximum critical load. This evidence will be shown in the numerical analyses reported in the next Section.

2.2. Interaction effects on imperfection sensitivity

The proposed system was considered as perfect, but real systems are always affected by defects and imperfections. The effect of the previously discussed interaction has an influence also in the structural behavior of imperfect structures. In a Von Mises Arch, considering an initial curvature for each hinged bar, the imperfection can be seen as an eccentricity of the centroid of the section from the straight axial line [20]. Traditionally, a sinusoidal curve is used to represent such imperfect configuration, thus the maximum eccentricity is located in the mid-span of every bar (Fig. 8). Such configuration is proportional to the first Eulerian buckled eigenshape. As a consequence, during a displacement control snap-through analysis, the bars are pushed to chase the bifurcation. Under these conditions, the actual equilibrium

Fig. 8. Possible imperfection patterns for a Von Mises Arch affected by a sinusoidal initial deflection.

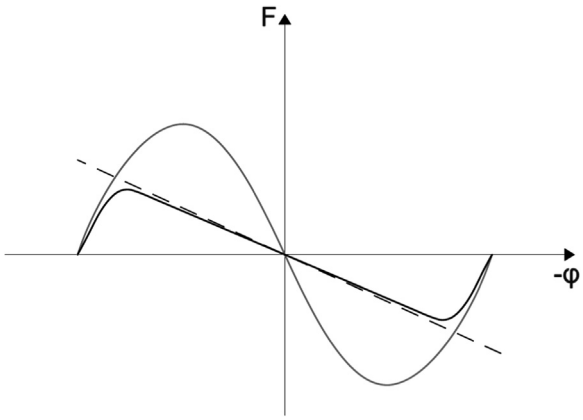

Fig. 9. Equilibrium path of a real system (black line) vs. the snap-through (grey line) and elastic buckling (dotted line) paths of a perfect system.

path moves away from the ideal one, and, the bifurcation degenerates to a limit point. Such point corresponds to the actual critical load of the system, and its value is always lower than the one related to the interaction phenomenon. From a qualitative point of view, this concept can be seen in Fig. 9, where the actual equilibrium path (imperfect system) results to be down-shifted by the elastic buckling branch; it means that the higher the initial curvature, the greater the load reduction. Under the light of this, the elastic buckling branch represents the envelope of the all the possible equilibrium paths of an imperfect system. The distance between each equilibrium path of a set of imperfect systems depends on how the interaction occurs. The load reduction increases with the imperfection magnitude, but this increasing it is obviously nonlinear. Thus, when the interaction is present, it is not possible to determine a priori the quantitative effect of the imperfection sensitivity on the load reduction.

Phenomenon of interaction cannot be neglected for a correct evaluation of the critical load of a geometrically nonlinear system; nevertheless, a classic nonlinear analysis led to an erroneous value of the actual critical load [21]. Recalling the definition of a displacement control analysis, the branch after a limit point of an equilibrium path can be followed, even if it is an unstable one. As a consequence, the interaction limit point is surpassed and the snap-though critical load is assumed as the critical one. Furthermore, the nonlinear bifurcation implicates a stronger imperfection sensitivity of the system in respect with the one of the same entity of defects but not affected by interaction [22].

3. Numerical simulations of the interaction effects

The results of the numerical analyses performed in order to confirm the phenomenon of interaction between different instability typologies were reported. As discussed at the end of the previous Section, the transition from an instability condition to another depends on the slenderness of the bars and the shallowness of the structure. A Von Mises Arch of semi-span $d=2,5\ m$ and variable height h was considered (Fig. 1). In the simulation, the cross section of the arch was realized by a tubular profile with a variable diameter in order to obtain different inertial properties (see Table 1). The following parameters were considered during the analyses: the slenderness λ, the shallowness ratio (h/d) and different imperfection patterns.

As far as the first two parameters is concerned, a large set of them were used, as reported in Table 2. Additionally, different imperfection schemes were adopted in order to evaluate the effect of their presence and their size: (*i*) no imperfections: straight bar; (*ii*) sinusoidal imperfection with maximum eccentricity equal to $L/300$; (*iii*) sinusoidal imperfection with maximum eccentricity equal to $L/1000$.

The elastic buckling can occur with a symmetric or asymmetric

Table 1
Cross section properties of the arch bar member.

D_{ext}	External diameter
D_{int}	Internal diameter
Thickness, s	$s = 0{,}06D_{ext}$
Cross Section Area, A	$A = \frac{\pi}{4}(D_{ext}^2 - D_{int}^2)$
Moment of Inertia, I	$I_y = I_z = \frac{\pi}{64}(D_{ext}^4 - D_{int}^4)$
Elastic Modulus, $E\left[\frac{N}{mm^2}\right]$	$E = 210E^9$
Poisson ratio, ν	$\nu = 0{,}3$

Table 2
Sets of λ and h/d parameters used for the numerical simulations.

Slenderness λ	**Shallowness ratio** $\frac{h}{d}$	**Arch depth** h **[m]**
20	0,02	0,05
40	0,04	0,10
60	0,06	0,15
80	0,08	0,20
100	0,10	0,25
120	0,12	0,30
140	0,14	0,35
160	0,16	0,40
180	0,18	0,45
200	0,20	0,50

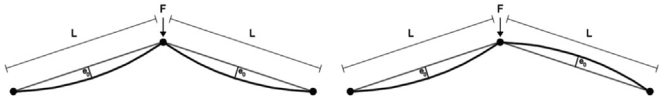

Fig. 10. Imperfection schemes applied for the numerical analyses: symmetric and asymmetric beams implementation.

eigenshape. Under this conditions, the imperfection must be applied both symmetrically and asymmetrically, as reported in Fig. 10.

All the numerical simulations were performed in a displacement control scheme, applying a vertical incremental displacement U at the top of the arch. A FEM solver engine was adopted using a co-rotational formulation and a geometrically nonlinear BTS3 beam element. In this section, equilibrium path will be displayed in terms of the vertical force F applied at the top and the vertical displacement U. Because the angle φ and displacement U are univocally related, the results remain entirely valid.

In order to obtain a validation of the theoretical formulations of Section 2, the results of the numerical analyses of a Von Mises Arch were reported. The snap-through is always present for such structural scheme, thus represent the perfect test structure for a given set of slenderness and shallowness ratios. As a first implementation a fixed value of λ=60 was chosen, and the shallowness ratio h/d was varied as reported in Table 1. Fig. 11a shows the equilibrium paths in the case of h/d ratio equal to 0,06 (h=0,15 m). It is evident that, for such structural configuration there is no interaction between snap-through and elastic buckling. $L/1000$ imperfection curve was not reported as it is practically coincident with the $L/300$ one. In Table 3, limit load values and percentage reductions from the perfect system load were reported for the three structural systems.

Table 3
Critical load values for λ=60 and h/d =0,06.

	F [kN]	**Variation** [%]
Perfect system	48,20	
L/1000 imperfection	47,99	– 0,43
L/300 imperfection	46,10	– 4,35

Table 4
Critical load values for λ=60 and h/d=0,08.

	F [kN]	**Variation** [%]
Perfect system	114,24	
L/1000 imperfection	112,29	– 1,71
L/300 imperfection	102,47	– 10,30

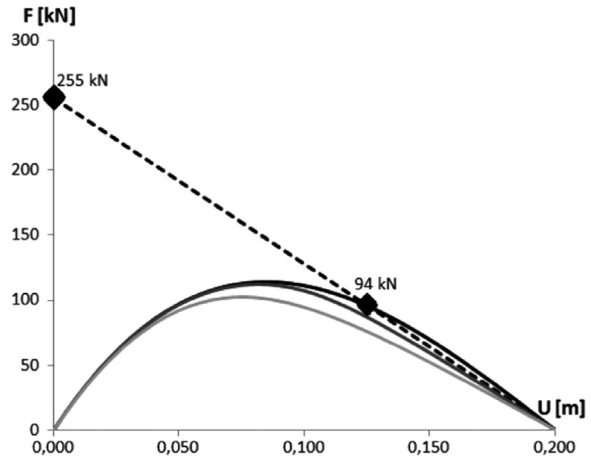

Fig. 12. Secondary equilibrium path (dotted line) related to elastic Eulerian buckling for λ=60 and h/d=0,08 in relation with the primary numerical equilibrium path of Fig. 11b. The imperfect systems are enveloped by the Eulerian buckling equilibrium path.

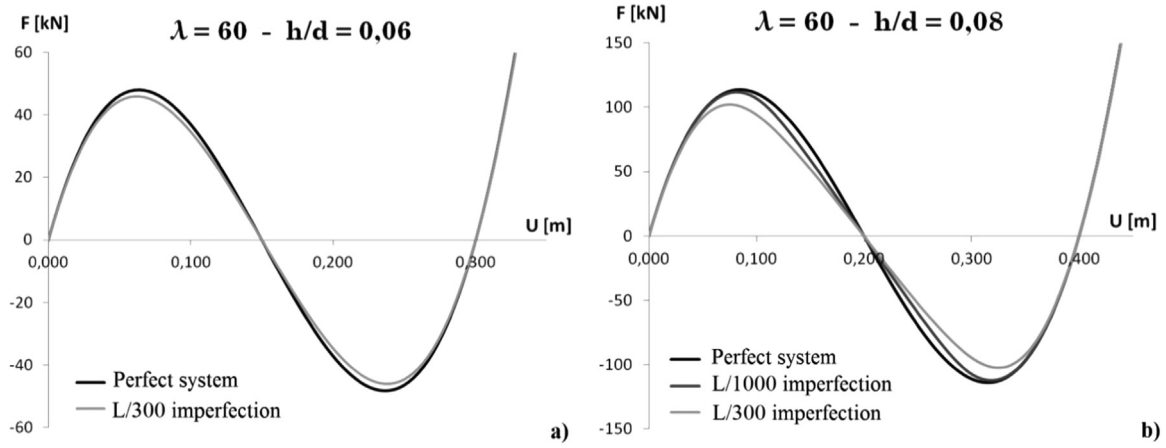

Fig. 11. Numerical equilibrium paths for two different h/d ratios and fixed λ.

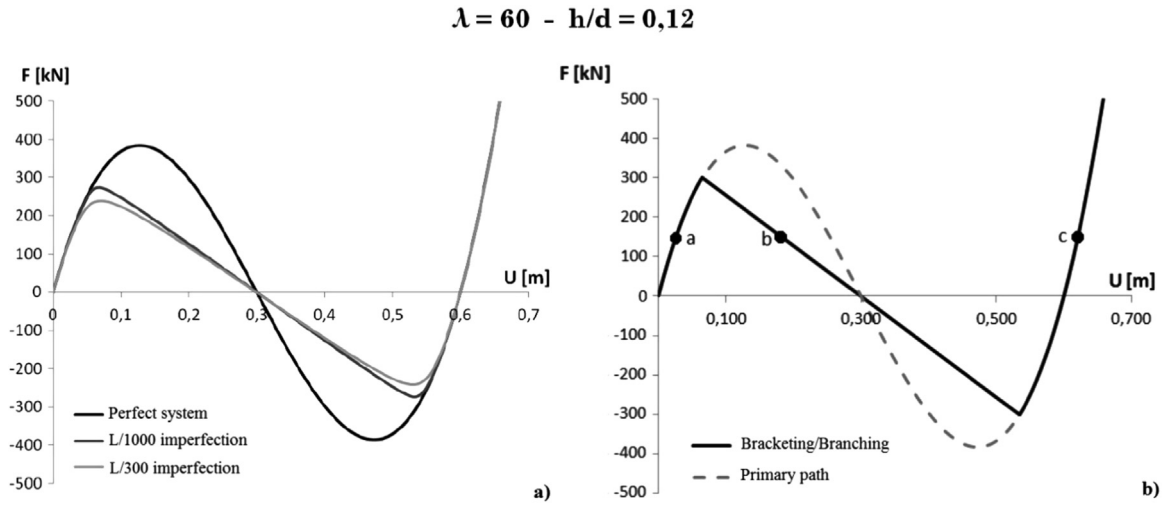

Fig. 13. a) Numerical equilibrium path for $\lambda=60$ and $h/d=0,12$. **b)** Bracketing and branching analysis for the same system.

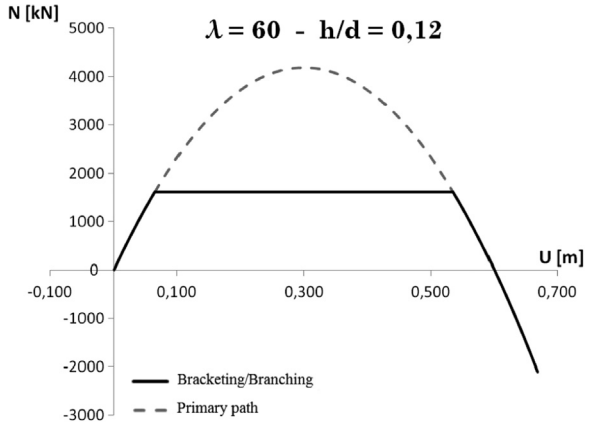

Fig. 14. Axial forces in the bars along the primary and bracketed equilibrium path.

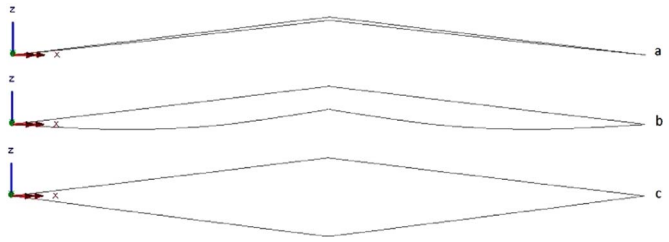

Fig. 15. FEM computed deformed configuration for the same external load value (150 kN), in three different position along the equilibrium path.

Table 5
Critical load values for $\lambda=60$ and $h/d=0,12$.

	F [kN]	**Variation from limit snap-through point** [%]	**Variation from intersection point** [%]
Perfect system	385,85		
Intersection point	301,10	– 21,96	
L/1000 imperfection	274,05	– 28,92	– 8,98
L/300 imperfection	239,69	– 37,83	– 20,40

Increasing h/d ratio up to 0,08 ($h=0,2\ m$), same results were reported in Table 4. Even this case, the interaction does not occur and the crisis takes place with the yielding of the limit point of the primary equilibrium path, as displayed in Fig. 11b.

It is worth to note that there is a gap in the decreasing branch between the equilibrium paths of the imperfect structure and the primary one. This means that the interaction occurs but the intersection with the elastic buckling secondary path is located beyond the limit point (see Section 2, Fig. 6c). Using the theoretical formulation as displayed in Section 2, it is possible to demonstrate the hypothesis. Expression (8), in terms of variable U, was overlapped to equilibrium paths, as shown by the dotted line in Fig. 12. It is obvious that for $U=0$ the curve provides the critical load value of a linearized Eulerian buckling analysis, in this case equal to *255 kN*; this can be verified by expression (1). The interaction occurs for a value of *94 kN* beyond the limit point, as a performed bracketing numerical analysis confirmed. Although the interaction does not represent a critical situation, it is evident that its presence influences the structural behavior along the decreasing branch, especially for the imperfect systems.

Operating in the same way for a less shallow structure, the system obviously acquires a larger strength with respect to vertical loads, but the interaction phenomena becomes prevalent. Fig. 13a shows the $F–U$ curves for an h/d ratio equal to 0,12. The critical load values of the imperfect systems is considerably lower than the ideal one. In this case a numerical bracketing analysis has been performed in order to identify the intersection point between the two equilibrium path. Then, by a branching procedure it was possible to follow the elastic buckling path (secondary one), as reported in Fig. 13b. In agreement with the theoretical expression, it is possible to observe that the equilibrium paths of the imperfect systems are below such numerical line; nevertheless, the intersection point could not be reached by the same systems. Considering now the axial forces in the bar (Fig. 14) it is possible to verify that the interaction has to be conferred to the yielding of the critical load value $N_{CR,EB}$, defined in Section 2, equal in this case to 1612 kN. It is worth to note that the system can have three possible different equilibrium configuration for the same level of external load, as indicated by the a,b and c points in Fig. 13b, related to a threshold value of 150 kN. In Fig. 14, the three corresponding deformed configuration are reported. In detail, it can be observed how following the secondary path (point b in Fig. 13b) the bars lose their rectilinear form in order to institute the equilibrium in the adjacent configuration (Fig. 15b). Once the overturn of the system (point c in Fig. 13b) has occurred, the bars were tensed and the straight configuration was recovered (Fig. 15c). If expression (10) of Section 2 is now considered, the value of the angle φ_{int} for which the interaction occurs can be evaluated. Its value, equal to 0,093775 rad, when substituted in expression (8) provides a maximum instability load equal to $F_{cr,int}$=299,09 kN, which differs from the one numerically evaluated ($F_{cr,int}$=301,10 kN) by less than 1%. Critical load values of the

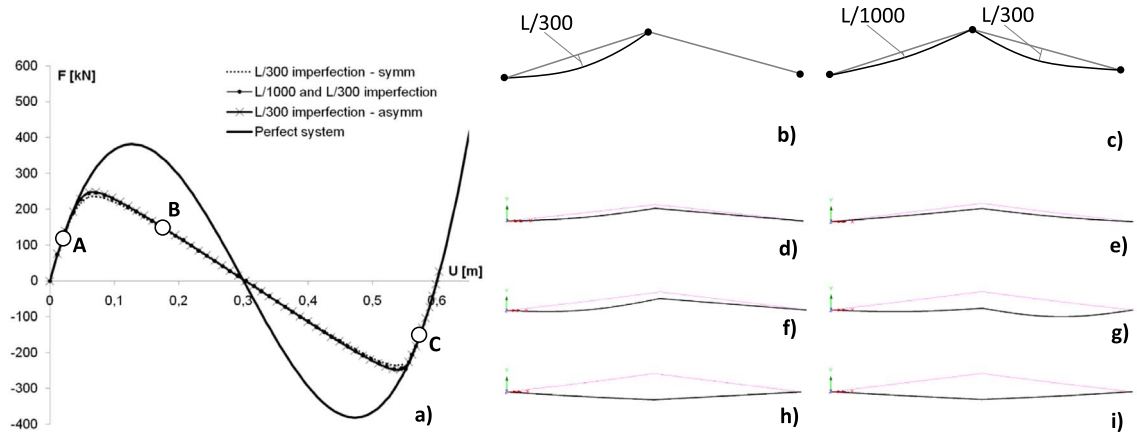

Fig. 16. a) Numerical equilibrium paths for the system represented in Fig. 11b with the addition of the asymmetric imperfection patterns. **b)** and **c)** Imperfection schemes applied for the numerical analysis. **d)** and **e)** Deformed shape of the arch at point A for the related imperfection scheme. **f)** and **g)** Deformed shape of the arch at point B for the related imperfection scheme. **h)** and **i)** Deformed shape of the arch at point C for the related imperfection scheme.

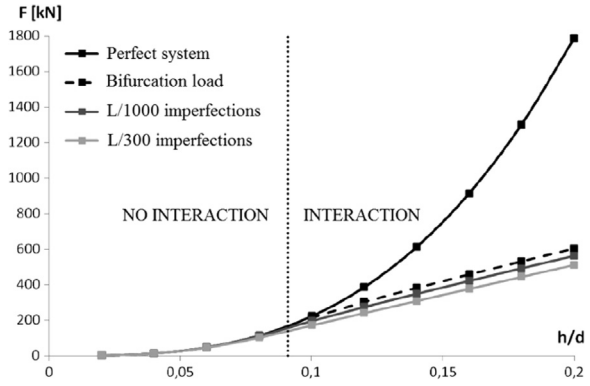

Fig. 17. Critical load reduction for an increasing h/d ratio and a fixed $\lambda=60$.

numerical analyses were summarized in Table 5, which indicates, in addition to the variation from the ideal snap-through limit value, even the percentage reduction from the intersection point (interaction load for the perfect system). Finally, the case of an asymmetric imperfection pattern was applied to this structural arrangement in two different way: (i) the L/300 deviation was present only in the left bar of the arch and (ii) both L/1000 and L/300 deviations were present to the left (Fig. 16b) and the right bar (Fig. 16c) respectively. Results, in terms of *F–U* curves were summarized in Fig. 16a together with the equilibrium path of the perfect system and the *L/300* symmetric imperfection evaluated above. As it can be observed, the *F–U* curves of the asymmetric imperfection patterns resulted to be coincident with the equilibrium path of the *L/300* symmetric deviation. This means that only the bar with the higher deviation governs the interaction phenomenon. The Eulerian buckling of the arch corresponds in fact with the Eulerian buckling of one of its beams, and a higher deviation signifies a nearest condition to the critical load. Since the system is subjected only to axial forces, the collapse of one of its element does not allow any internal force redistribution and the arch goes towards a snap-through instability. In Figs. 16d and e the computed deformed shapes of the two asymmetric deviations at Point A of the equilibrium path in Fig. 16a were respectively reported. Interaction has not occurred yet and the system lowers itself with an asymmetrical shape and the two bars have different displacements field [16]. Analyzing the same deformed shapes at Point B (Figs. 16f and g respectively), it is possible to observe that the equilibrium has been achieved in the adjacent configuration for the *L/300* deviated bars. In the case of no imperfections for one of the beams, the rectilinear configuration was maintained through all the nonlinear bifurcation branch (Fig. 16f). In Figs. 16h and i, the deformed shapes at Point C were reported. The inversion of the compressive regime to a tensile regime of internal forces, makes impossible the achievement of the equilibrium with a deviated configuration of the beams and in both of the cases the rectilinear configuration of all bars was recovered.

It is evident from these results, that the interaction phenomenon makes necessary a structural analysis considering the presence of imperfections; nevertheless, the overestimation error would be even larger if the non-linear bifurcation is neglected.

All the analyses discussed were repeated for all the values of h/d ratios of Table 1 and for a fixed value of λ equal to *60*. Results were reported in Fig. 17, showing that the critical loads reduction increases as the shallowness decreases. It is interesting to observe that, when the interaction is present, the limit load of imperfect systems increases linearly with the h/d ratio. This happens because the nonlinear bifurcation load has the same trend, as reported by the dotted lines in Fig. 17. These results are of a remarkable importance: they define two different, but essential, concepts.

Firstly, the interaction phenomenon has a threshold value which represents the least burdensome condition for the structure. Moving away from the interaction boundary configuration, structural behavior gets worse in terms of the actual explicable strength with respect to potential strength. Secondly, the presence of the imperfections is more significant than their magnitude for the limit load reduction of a structural configuration affected by the interaction. This is clear in Fig. 16, where there is a minor distance between the two imperfect systems curves, although their difference in terms of imperfection magnitude is substantial.

Until now, a fixed value of λ equal to 60 was used in order to determine the effect of the interaction with respect to the shallowness. However, the same analyses can be repeated with a variable slenderness and a fixed h/d ratio. To this purpose, a system with h/d ratio equal to 0,08 ($h=0,2$ *m*) was chosen and a set of λ, as shown in Table 2, was used. In Fig. 18, the equilibrium paths for three λ values from 40 to 140 were reported. The increasing of the slenderness implies a reduction of the arch buckling strength. As a consequence, the arch is more sensitive with respect to the instability interaction, as can be seen by the significant load reduction in Fig. 18c. Under the light of this, the critical loads for an increasing value of λ and a fixed value of h/d ratio (equal to 0,08) were reported. The analogous graph of Fig. 17 was obtained. It is worth to note that the increasing of the variable parameter (λ) is now related to the decreasing of the critical load, on the opposite to the increasing of h/d ratio. As a consequence, the larger reductions are located in the zone where the absolute magnitude of the critical loads are lower. The larger distances between the imperfect systems curves comes for λ over than 80. This happens because for slenderness lower than 80, the effect of the interaction is less influential

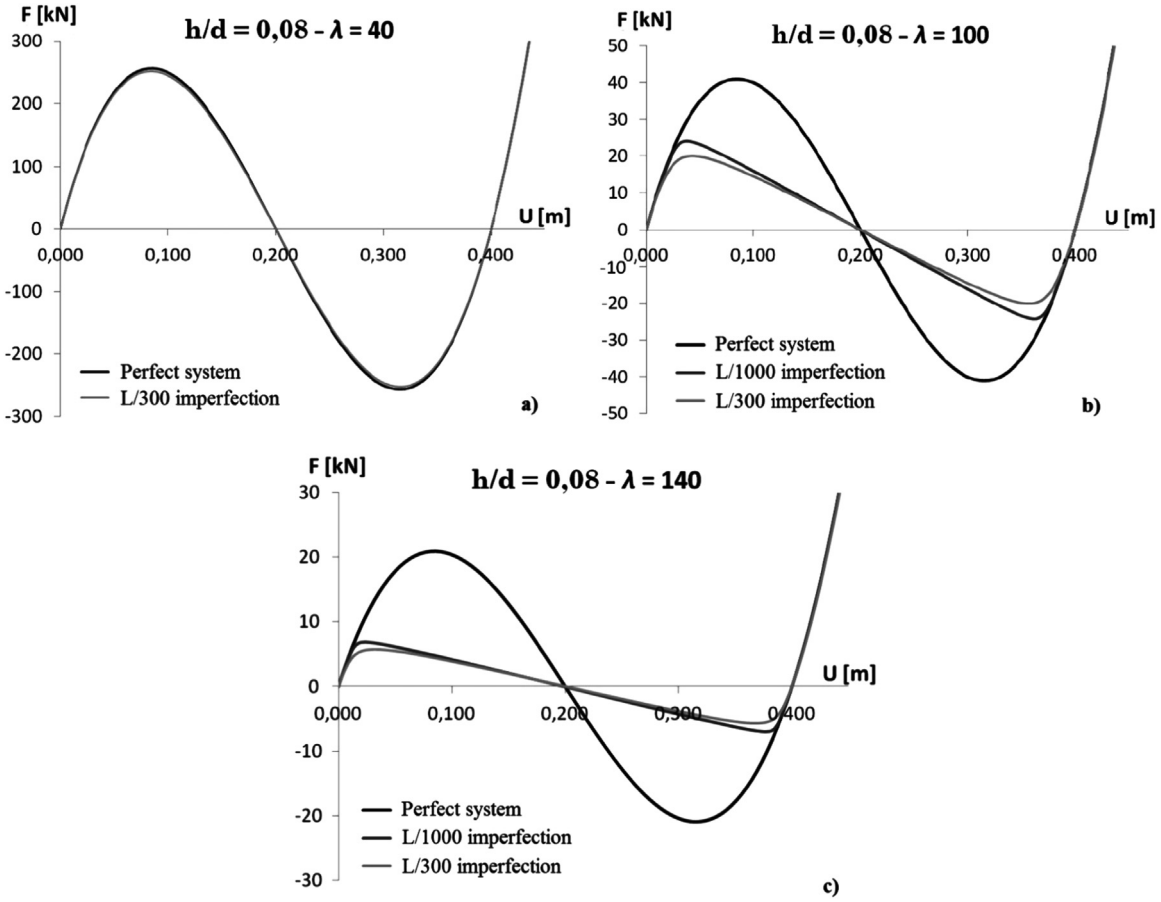

Fig. 18. Numerical equilibrium path for three different structural arrangement with a fixed *h/d* ratio and variable λ.

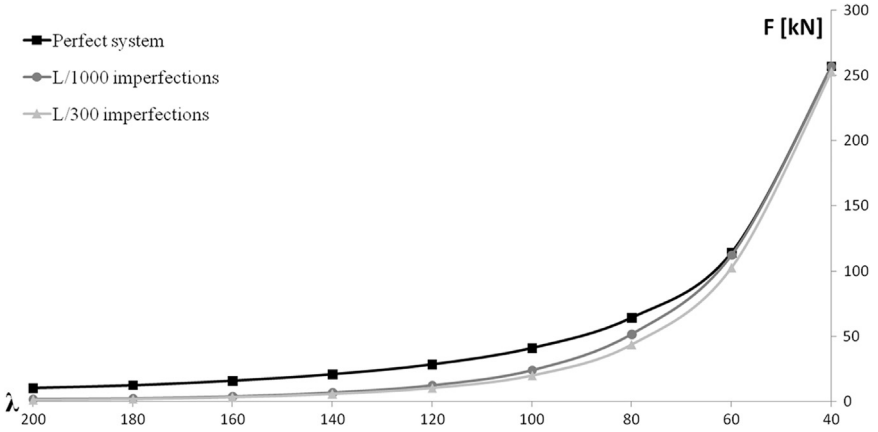

Fig. 19. Critical load reduction due to different imperfection patterns for an increasing λ and a fixed *h/d* ratio equal to *0,08*.

and the load reduction must be associated only to the size of the imperfections. As a consequence, the same observations of Fig. 17 can be done. The most burdensome condition occurs when the effect of the interaction becomes primary and the imperfections are present. In addition, the interaction condition represents the boundary of a structural configuration in order to exclude substantial load reductions due to the imperfections. This results are in total agreement with the theoretical formulation of the interaction curve, obtained in Section 2 (Fig. 7). It is worth to note that for λ values larger than 140, the critical elastic buckling load is very low, then the imperfection sensitivity becomes secondary with respect to the interaction phenomenon. This is clear in Fig. 19, where the two curves related to the imperfect systems are practically overlapped in the high λ zone. At the same time, this coincidence was observed for the minimum values of λ, thus where the interaction cannot take place (λ lower than 40).

4. Conclusions

In the present study, an original approach to evaluate the interaction between different instability typologies was proposed for slender and elementary shallow structures. For the first time, a theoretical interaction curve was obtained (Eq. (10), Fig. 7). This result permitted to define the existence domain of the interaction phenomenon in term of inertial and geometrical properties of a structure. In addition, the proposed approach allowed to determine the dangerousness of a certain structural configuration in terms of critical load reduction as

reported in Section 3. This was possible by the distance evaluation between the considered system and the interaction boundary curve (Fig. 7). Results confirmed that the reductions for the critical load were consistent, and, for some cases equal to the 40% of the critical load computed by buckling or snap-through analysis separately.

A parametric set of numerical analyses for a large number of slenderness and shallowness ratios was conducted in order to confirm and verify the theoretical results for a Von Mises arch. On the one hand, when the h/d ratio is high, the interaction phenomenon was observed, and the related critical load reductions were substantial. On the other hand, same results were obtained with small values of λ, but with a critical load reductions less significant because the critical loads were lower in terms of magnitude. The numerical simulations reported in Section 3 proved the validity of the theoretical formulation. Critical load reductions appeared to be consistent with the expressions obtained by the closed form solution, and values of the 40% of the critical load (the minimum between buckling and snap-through analysis) were found. In addition, the expected physical structural behavior was observed in the numerical models, and the deformation time history analysis was in agreement with the theory.

At the same time, the interaction effect on the imperfection sensitivity was evaluated. In order to do it, two different imperfection schemes (*L/300* and *L/1000*) were applied on the structures. Equilibrium paths of the imperfect systems were evaluated, and, as expected, the interaction appeared to intensify the imperfection sensitivity. The additional load reduction, numerically computed, must to be attributed to the interaction. This happens because the considered imperfection pattern forced the structure to follow the secondary equilibrium path from the first loading steps. Furthermore, it has been found that an asymmetric pattern of imperfections have no effects on the interaction because the phenomenon is always governed by the beam element that first buckles. Finally, the effect of the magnitude of imperfections was evaluated. When the system laid on the interaction curve, the effect of the magnitude was very important. The system was characterized by the worst instability condition and the relative deviation due to the imperfection was substantial. Although, when the system was far from the interaction curve, but still in the interaction zone, the magnitude of the imperfections became to be secondary respect to their presence. In this case, the interaction effect was strong, and just a small perturbation led the system to nonlinear bifurcation.

As the conclusion, the presented approach underlines the importance of the interaction phenomenon, and its possible existence must be always checked. If a structure can suffer this occurrence, the imperfections must be accounted in all the structural analyses since their effect can be very high on the maximum tolerable design load. The challenge now is to extend the results to more articulated structures. The findings of this study have a number of important implications for future practices, in terms of structural design/analysis guidelines and advancement in researching snap-instability of structures.

Acknowledgements

Special thanks are due to Eng. Stefano Pescetelli for the precious work [23] done during his Master Thesis project.

References

[1] W.T. Koiter, The Stability of Elastic Equilibrium, 1970.
[2] P. Van Musschenbroek, Physicae Experimentales et Geometricae, Luchtmans, Netherlands, 1729.
[3] L. Euler, Mechanica Sive Motus Scientia Analytice Exposita, St. Petersburg, 1736.
[4] J.M.T. Thompson, Basic principles in the general theory of elastic stability, J. Mech. Phys. Solids 11 (1963) 13–20.
[5] J.M.T. Thompson, Towards a general statistical theory imperfection-sensitivity in elastic post-buckling, J. Mech. Phys. Solids 15 (1967) 413–417.
[6] K. Huseyin, Fundamental principles in the buckling of structures under combined loading, Int. J. Solids Struct. 6 (1970) 479–487.
[7] K. Huseyin, The elastic stability of structural systems with independent loading parameters, Int. J. Solids Struct. 6 (1970) 677–691.
[8] K. Huseyin, The stability boundary of systems with one degree of freedom (Part I), Meccanica 5 (4) (1970) 308–311.
[9] K. Huseyin, The stability boundary of systems with one degree of freedom (Part II), Meccanica 5 (4) (1970) 312–316.
[10] V. Gioncu, General theory of coupled instabilities, Thin-Walled Struct. 19 (1994) 81–127.
[11] D.A. Pecknold, J. Ghaboussi, T.J. Healey, Snap-through and bifurcation in a simple structure, J. Eng. Mech. 111 (7) (1985) 909–922.
[12] V. Gioncu, Consistent simplified theory for elastic coupled instability, Thin-Walled Struct. 19 (1994) 147–159.
[13] M. Rhodes, M.M. Jr. Mikulas, Deployable controllable geometry truss beams, in: NASA Technical Memorandum, Langley Research Centers, VA, 1985.
[14] K. Miura, Variable geometry truss concept, Inst. Space Astronaut. Sci. Rep. 614 (1984) 1–17.
[15] N. Hu, Buckling-induced smart applications: recent advances and trends, Smart Mater. Struct. 24 (6) (2015) 063001.
[16] M. Kalina, Numerical analysis of buckling of von mises planar truss, transactions of the VŠB – Technical University of Ostrava, Civ. Eng. Serv. 15 (2) (2016).
[17] T. Schioler, S. Pellegrino, Space frames with multiple stable configurations, AIAA J. 45 (7) (2007) 1740–1747.
[18] R. Von Mises, Uber die Stabilitatsprobleme der Elastizitatstheorie, ZAMM (1923) (406–402).
[19] P.X. Bellini, The concept of snap-buckling illustrated by a simple model, Int. J. Nonlinear Mech. 7 (6) (1972) 643–650.
[20] A. Carpinteri, R. Malvano, A. Manuello, G. Piana, Fundamental frequency evolution in slender beams subjected to imposed axial displacements, J. Sound Vib. 333 (2014) 2390–2403.
[21] A. Carpinteri, F. Bazzucchi, A. Manuello, Nonlinear instability analysis of -Long span roofing structures: the case study of Porta Susa railway station, Eng. Struct. 110 (2015) 48–58.
[22] Z.P. Bazant, L. Cedolin, Stability of Structures, World Sci. (2010) 2010.
[23] S. Pescetelli, Problemi di interazione tra instabilità di diversa specie nelle coperture reticolari (Ms. Thesis), Politecnico di Torino, Torino, Italy, 2014.